Model Spectra of Neutron Star Surface Thermal Emission

Lun-Wen Yeh, Gwan-Ting Chen, Hsiang-Kuang Chang

Department of Physics and Institute of Astronomy, National Tsing Hua University, Hsinchu, Taiwan 300 R.O.C.

Abstract

Many neutron star spectra reveal a thermal origin in the soft X-ray band, such as those of some radio pulsars (particularly of the middle-aged gamma-ray pulsars), and of radio-quiet isolated neutron stars. The thermal emission is believed to come from the atmospheres of neutron stars and it carries valuable information of physical properties of the surface. We construct a neutron star atmosphere model with the surface magnetic field of 10^{11} to 10^{13} gauss and the effective temperature of several million Kelvin. The fully ionized hydrogen with ideal gas equation of state is used for the composition of atmosphere. The radiative transfer equation is solved for two polarization modes in the plane-parallel and the radiative equilibrium atmosphere with opacities due to thermal bremsstrahlung and Thomson scattering only. We compute the radiative transfer equation with full angle-dependence of both photon polarization modes and the orientation of magnetic filed can be arbitrary in our model. For comparison we also solve the radiative transfer equation using the diffusion approximation. We discuss spectra, beaming patterns and temperature profiles for different field orientations. Near the electron cyclotron frequency the absorption feature in spectra for both polarization modes are apparent. The next step for our model is to include the opacities that have higher harmonics. We would like to explore the absorption features, which are observed in the spectrum of 1E 1207.4-5209 and some other sources.

Physical assumptions and solving radiation transfer equation

We constructed a plane-parallel neutron star atmosphere with strong magnetic field 10^{11} to 10^{13} gauss in the radiative equilibrium. We assumed the composition of atmosphere is the fully ionized hydrogen ideal gas. The typical effective temperature is about several million Kelvin hence only Thomson scattering process and the thermal bremsstrahlung are included in our model. In such strong magnetic field the radiation has two polarization modes, the ordinary mode (O-mode) and the extraordinary mode (X-mode), the properties for both mode are in results and discussions.

We use the gray temperature profile as first trial profile and the Oppenheimer-Volkoff equation for the hydrostatic equilibrium to solve the structure of atmosphere.

$$T^4 = \frac{3}{4} T_e^4 \left(\tau + \frac{2}{3} \right)$$

$$\frac{dP}{dz} = \frac{-\rho G m}{z^2} \left(1 + \frac{P}{\rho c^2}\right)\left(1 + \frac{4\pi z^3 P}{m c^2}\right)\left(1 - \frac{2Gm}{z c^2}\right)^{-1}$$

$$\Rightarrow \frac{dP}{dz} = -\rho g^*$$

$$\Rightarrow \frac{dP}{d\tau} = \frac{g^*}{\kappa_{sc}}$$

We define Thomson depth $d\tau = -\rho\kappa_{sc} dz$, where κ_{sc} is Thomson scattering opacity in the absence of magnetic field. In the assumption of LTE the radiation transfer equation is

$$\mu_R \frac{dI_\nu^i(\tau, \hat{k})}{d\tau} = \frac{[\kappa_{ff,\nu}^{*i}(\tau, \hat{k}) + \kappa_{sc,\nu}^i(\tau, \hat{k})]}{\kappa_{sc}} I_\nu^i(\tau, \hat{k}) - \frac{\kappa_{ff,\nu}^{*i}(\tau, \hat{k})}{\kappa_{sc}} \frac{B_\nu(\tau)}{2} - \frac{1}{\kappa_{sc}} \sum_{j'} \int \frac{d\kappa_{sc,\nu}}{d\Omega}(i, \hat{k} \leftarrow j', \widehat{k'}) I_\nu^{j'}(\tau, \widehat{k'}) d\Omega'$$

,where $\kappa^j_{sc,\nu}$ is Thomson scattering opacity and $\kappa^{j*}_{ff,\nu}$ is the reduced thermal bremsstrahlung opacity for j-mode (j=X or O), B_ν is the Planck function, $d\kappa_{sc,\nu}/d\Omega$ is the differential Thomson scattering opacity. The form of $d\kappa_{sc,\nu}/d\Omega$ and $\kappa^{j*}_{ff,\nu}$ are

$$\frac{d\kappa_{sc,\nu}}{d\Omega}(k, i \leftarrow k', j') = \frac{1}{m_p}\left(\frac{e^2}{m_e c^2}\right)^2 \left| \frac{1}{1+u^{1/2}} e_+^{i*} e_+^{j'} + \frac{1}{1-u^{1/2}+i\gamma} e_-^{i*} e_-^{j'} + e_z^{i*} e_z^{j'} \right|^2$$

$$\kappa_{ff,\nu}^{*j} = \kappa_{ff}^* \left[\frac{1}{(1+u^{1/2})^2} |e_+^j|^2 g_\perp + \frac{1}{(1-u^{1/2})^2 + \gamma^2} |e_-^j|^2 g_\perp + |e_z^j|^2 g_\parallel \right] \qquad u = \frac{\omega_c^2}{\omega^2}$$

,where e^j_+, e^j_-, e^j_z are the polarizations of radiation for j-mode which are derived in the assumption of the cold plasma dielectric tensor, $g_\perp$ and $g_\parallel$ are the gaunt factors. We included the radiation damping γ in the second term of opacities to avoid diverging as the photon frequency ω is equal to electron cyclotron frequency ω_c. The Feautrier method (Mihalas 1978) was adopted to solve the radiation transfer equation and we implemented the improved Feautrier method to reduce numerical round-off errors (Rybicki & Hummer 1991). In the radiative equilibrium the constraint of the radiation transfer equation is that the total flux must conserve. We used Unsold Lucy process (Mihalas 1978) to achieve the constant total flux. We use equal logarithmic grids in the depth and the frequency space ($\Delta\log\tau$=0.05 and $\Delta\log\nu$=0.1).

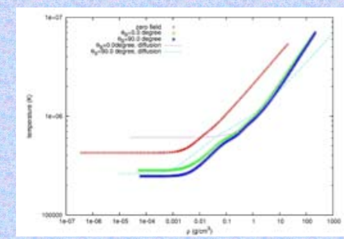

Fig.1. The temperature profiles of the atmosphere for zero field and B=10^{12} gauss as $T_{eff}=10^6$ K. θ_B is the angle between the surface normal and the magnetic field. We also show the results using the diffusion approximation for comparison.

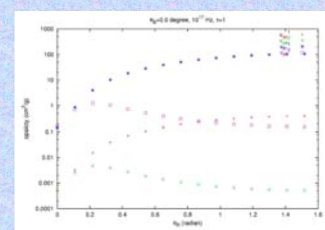

Fig.2. The opacities versus θ_R of 10^{17} Hz photon frequency and $\theta_B=0^0$ at τ=1. θ_R is the angle between the surface normal and the specific intensity.

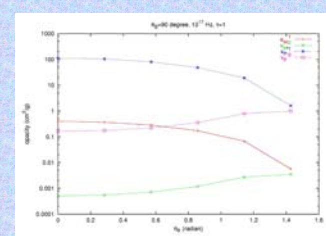

Fig.3. The opacities versus θ_R of 10^{17} Hz photon frequency and $\theta_B=90^0$ at τ=1. θ_R is the angle between the surface normal and the specific intensity.

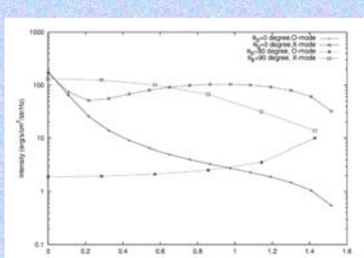

Fig.4. The beaming patterns of B=10^{12} gauss for $\theta_B=0^0$ and $\theta_B=90^0$. θ_R is the angle between the surface normal and the specific intensity.

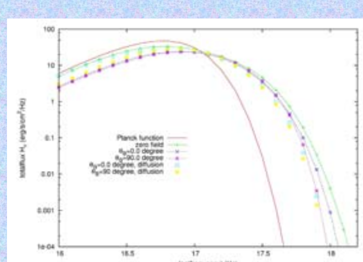

Fig.5. The spectra of Planck function, zero field and B=10^{12} gauss. θ_B is the angle between the surface normal and the magnetic field. The effective temperature is 10^6 K. We also show the results using diffusion approximation for comparison.

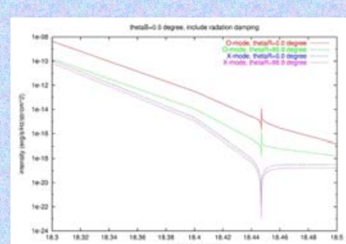

Fig.6. The spectra near the electron cyclotron frequency for both polarization modes. The radiation damping term is included in the opacities. θ_B is the angle between magnetic field and surface normal; θ_R is the angle between specific intensity and surface normal.

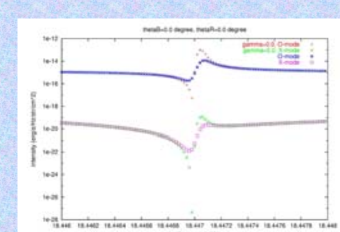

Fig.7. The spectra near the electron cyclotron frequency for both polarization modes. The effect of the radiation damping term gamma is compared. θ_B is the angle between magnetic field and surface normal; θ_R is the angle between specific intensity and surface normal.

Results and discussions

In the 10^6 K effective temperature Fig. 1 shows the temperature profiles for zero field, $\theta_B=0^0$ and B=10^{12} gauss, $\theta_B=90^0$ and B=10^{12} gauss. The flat features at outer layer in all temperature profiles can extend as the density decreases which is the result from the plane-parallel geometry. The emergent intensity of zero field mainly come from more deep layer than that of B=10^{12} gauss. The reason is that the magnitude of opacities are reduced in the strong magnetic field hence the atmosphere appear optically thin for strong field than zero field. The temperature profiles of strong magnetic field have plateaus near $\rho=10^{-3}$ to 1 g/cm^3. Those plateaus are because the O-mode photons decouple with matter at more outer atmosphere than X-mode photons and the angle-dependence of O-mode photons is stronger than that of X-mode photons. The temperature at most outer layer of $\theta_B=0^0$ is higher than that of $\theta_B=90^0$ hence in our model the surface temperature at the magnetic pole is higher than the surface temperature of the equator. The angle-dependence of Thomson scattering and the thermal bremsstrahlung opacities for both polarization modes at τ= 1 are shown in Fig.2 and Fig.3. If the angle between the magnetic field and the specific intensity is zero, both photon polarization modes have circular polarizations therefore the opacities are small. If the angle near 90 degree, the polarization direction of O-mode photons mainly lies on the plane formed by magnetic field and specific intensity which result in large opacities; the polarization direction of X-mode photons is mainly perpendicular to the plane hence the opacities are small. The beaming pattern are showed in Fig. 4 and the behavior can be explained by Fig. 2 and Fig. 3 that means the effect of limb darkening is tiny for the beaming patterns of both polarization modes. The spectra of zero field and B=10^{12} gauss are harder than Planck function at high energy part that is because high energy photons originate from more deep atmosphere (Fig. 5). An absorption feature in the X-mode spectrum around the electron cyclotron frequency is as anticipating (Fig. 6). The absorption feature in the O-mode spectrum around the electron cyclotron frequency is because of the incoming X-mode polarization photons due to differential Thomson cross section (Fig. 6). The shape of the absorption line depends on damping terms in the opacities. We compare the absorption feature with the radiation damping and without the radiation damping (Fig. 7). We only included the radiation damping term here, considering the collision damping and thermal damping are necessary in our future work. Based on these works we will include higher harmonic of electron cyclotron resonance in order to study the spectra of 1E1207.4-5209 and some other sources with absorption features.

References

Kaminker A.G., Pavlov G.G., Shibanov Yu. A., 1982, Ap&SS, 86, 249
Mihalas, D., 1978, Stellar Atmosphere. 2nd edn. W.H. Freeman and Co., San Francisco
Rybicki, G.G., Hummer, D.G., 1991, A&A, 245, 171
Wynn C.G.Ho, Dong Lai, 2001, MNRAS, 327, 1081